Preprint typeset using LaTeX style emulateapj v. 6/22/04

THE FIRST POLARIMETRIC SIGNATURES OF INFRARED JETS IN X-RAY BINARIES

T. Shahbaz[1,2], R.P. Fender[3], C.A. Watson[4], K. O'Brien[5]

ABSTRACT

We present near-infrared linear spectropolarimetry of a sample of persistent X-ray binaries, Sco X–1, Cyg X–2 and GRS 1915+105. The slopes of the spectra are shallower than what is expected from a standard steady-state accretion disc, and can be explained if the near-infrared flux contains a contribution from an optically thin jet. For the neutron star systems, Sco X–1 and Cyg X–2, the polarization levels at 2.4μm are 1.3±0.10% and 5.4±0.7% respectively which is greater than the polarization level at 1.65μm. This cannot be explained by interstellar polarization or electron scattering in the anisotropic environment of the accretion flow. We propose that the most likely explanation is that this is the polarimetric signature of synchrotron emission arising from close to the base of the jets in these systems. In the black hole system GRS 1915+105 the observed polarization, although high (5.0±1.2% at 2.4 μm), may be consistent with interstellar polarization. For Sco X–1 the position angle of the radio jet on the sky is approximately perpendicular to the near-infrared position angle (electric vector), suggesting that the magnetic field is aligned with the jet. These observations may be a first step towards probing the ordering, alignment and variability of the outflow magnetic field in a region closer to the central accreting object than is observed in the radio band.

Subject headings: accretion: accretion discs – binaries: close stars: individual (Sco X–1, Cyg X–2, GRS 1915+105)

1. INTRODUCTION

In the past decade or so overwhelming evidence has pointed to a clear coupling between accretion and the formation of relativistic jets in galactic X-ray binary systems (see Fender 2006). Accretion states associated with hard X-ray spectra appear to be associated with the production of a relatively steady, continuously replenished and partially self-absorbed outflow (Fender 2001), while major outbursts are associated with more discrete ejection events which may be resolved and tracked with radio interferometers (e.g. Mirabel & Rodriguez 1994).

In the radio band the steady jets observed during the hard X-ray states have a flat ($\alpha \sim 0$, where $S_\nu \propto \nu^\alpha$) spectrum, probably resulting from self-absorption in a self-similar outflow (e.g. Blandford & Konigl 1979). Above some frequency this flat spectral component should break to an optically thin spectrum ($\alpha \sim -0.6$) corresponding to the point at which the entire jet becomes transparent. There is some evidence from some black hole X-ray binaries that this break occurs around the near-infrared spectral region (e.g. Corbel & Fender 2002; Nowak et al. 2005; Homan et al. 2005; Russell et al. 2006), something which can be well fit by jet models (Markoff et al. 2001; Markoff et al. 2003). Thus the case is strong that there is a significant contribution of synchrotron emission, probably optically thin, in the near-infrared spectral regimes of X-ray binaries. However, one key test which is yet to be reported is a measurement of the linear polarization in this regime. Not only would a high level of linear polarization confirm the synchrotron interpretation, it would offer us the opportunity to study the degree of ordering and orientation of the magnetic field at the base of the jet. In this paper we present near-infrared spectropolarimetry for a sample of luminous X-ray binaries, all of which can be confidently identify as jet sources based on radio observations.

2. OBSERVATIONS AND DATA REDUCTION

We obtained HK spectropolarimetry of three X-ray binaries Sco X–1, Cyg X–2 and GRS 1915+105 with UKIRT during the nights of 18, 19, 22 and 23 July 2004. UIST was used with the HK (1.4μm–2.5μm) grism and the InSb array with a 2 pixel wide slit, giving a spectral resolution of 680 km s^{-1} at 2.2μm. We used the IRPOL2 polarimetry module which comprises of a half-wave retarder, a focal plane mask and a Wollaston prism which splits the light from each aperture mask into orthogonally polarized ordinary (o-) and extraordinary (e-) beams which are then projected onto the array. Rotating the half-wave retarder to 0.0°, 45°, 22.5° and 67.5° allowed us to obtained spectropolarimetry. The normalized Stokes parameters are then determined from ratios of the two intensities measured in each frame, canceling any changes in sky transmission between images.

To determine the polarization spectrum we took short exposures of the target and sky pair (obtained by nodding the target along the slit) at the four half-wave retarder positions giving rise to 8 spectra of the target and a measurement of the polarization state of the target. The target spectra were proceeded by observations of an F or A-star, which were used to remove the telluric atmospheric features. Furthermore, observations of a non-polarized object and a polarized object were observed to determine the instrumental polarization level and positional angle. A journal of observations is presented in Table 1

[1] Instituto de Astrofísica de Canarias, 38200 La Laguna, Tenerife, Spain
[2] tsh@iac.es
[3] School of Physics and Astronomy, The University of Southampton, Southampton, SO17 1BJ, UK
[4] Department of Physics and Astronomy, University of Sheffield, Sheffield, S3 7RH, England
[5] European Southern Observatory, Alonso de Corovo, Santiago, Chile

The ORAC-DR pipeline was used to reduce the data, extract the spectra and determine the polarization state of the targets. First the bad pixel mask was applied and then the images were dark-subtracted, flat-field and sky-subtracted. The o- and e- beams were then optimally extracted (which also allows for any slight spectral tilt) and wavelength calibrated using the Argon arc (rms error of 1.7$\AA$). Lazzati et al. (2003) have noted that the values of the shape of the polarization spectrum can depend on the the extraction technique. We used different methods (optimal, normal extraction and tracing) and find no such dependancy. POLPACK was then used to determine the intensity I and the Stokes Q and U vectors. The flux calibration was done by using the telluric star. The target spectra were divided by the telluric star (with the stellar features interpolated), and then multiplied by the flux of the telluric star, determined from a blackbody function with the same effective temperature and flux as the telluric star.

3. SPECTRA

In Figure 1 we show the dereddened HK spectra of Sco X–1, Cyg X–2 and GRS 1915+105 using colour excess $E(B-V)$ values of 0.3 (Vrtilek et al. 1991), 0.4 (Orosz & Kuulkers 1999) and 6.3 (Chapuis & Corbel 2004) respectively and the extinction law from Howarth (1983). The H and K slit-magnitudes obtained after integrating the spectra with the filter responses are as follows; H=11.6, K=11.5 for Sco X–1, H=13.2, K=13.0 for Cyg X–2 and H=11.7, K=11.4 for GRS 1915+105. The dereddened spectra can be described as a power-law ($F_\nu \propto \nu^\alpha$) with indicies of 1.46±0.04, 0.98±0.02 and 1.21±0.05 for Sco X–1, Cyg X–2 and GRS 1915+105 respectively. The slopes are not consistent with what is expected from a standard steady-state accretion disc (index of 1.5; Bandyopadhyay et al. 1999). Indeed the slopes are shallower and can be explained if the near-infrared flux contains a contribution from an optically thin jet.

4. POLARIZATION

For each target we obtain eight spectra for each single set of observations of a target star. At each of the four wave-plate angles, we measure the flux in the two orthogonal (o- and e-) polarizations. These measurements are combined to produce the normalized Stokes q ($=Q/I$) and u ($=U/I$) spectra. The polarization spectrum p and position angle θ is then be calculated using $p=\sqrt{q^2+u^2}$ and $\theta = 0.5\tan^{-1}(u/q)$ respectively. The Stokes parameters may contain some component of instrumental polarization introduced by reflections within the telescope and detector optics. The instrumental polarization was determined from the non-polarized standard star observed each time the science target was observed, and was typically $< 0.1\%$.

The level and quality of the polarization spectra were not sufficient enough to allow us to resolve the variations in the polarization level across the major emission lines. The only reliable information that could be extracted was the continuum. In Figure 2 we show the wavelength binned polarization spectrum for our targets. For Sco X–1 we could not determine θ on UT 20040719 and so the polarization of the source was not detected. Hence we only averaged the individual Stokes q and u vectors on UT 20040718 and 20040723 before calculating the polarization spectrum. As one can see, Sco X–1 and Cyg X–2 both show polarization spectra that increase at longer wavelengths (lower frequencies) i.e. the 2.4μm polarization is larger than the 1.65μm polarization level. For GRS 1915+105 the opposite is the case. In order to demonstrate that the trends observed in our science targets are genuine, we also show the polarization spectrum of a polarized standard star HD183143 determined in exactly the same way as for the science targets. The polarization spectrum is as expected (Gehrels 1974). In Table 2 we give the polarization and position angle values. Although the polarization standard HD183143 can be used as a validation of the data reduction method, the standard is bright while the targets are faint, close to the sky background level, and so poor sky subtraction may introduce a correlation between target brightness and polarization level. However, it should be noted that Sco X–1 and GRS 1915+105 have similar magnitudes but very different levels of polarization. To calculate the mean polarization at 1.65μm and 2.4μm, we assume that the Stokes vector do not change over 0.10μm (N=90 pixels). We can thus calculate the mean Stokes q and u vectors and determine the mean polarization. The uncertainty on these values is then the standard error, given that we have N individual measurments of q and u respectively. The uncertainty in the mean polarization and position angle then follows by propagating the errors on q and u. Given that our final mean polarization values are significant (note that we average over 90 pixels) a bias correction (Simmons & Stewart 1985) is not necessary, as pointed out by Jensen et al. (2004).

4.1. *Sco X–1*

Sco X–1 has a colour excess of $E(B-V)$=0.3 so some interstellar polarization is expected. Schultz, Hakala, & Huovelin (2004) fit the UBVRI optical linear polarization values with the empirical formula of Serkowski ($P(\lambda) = P_{\rm max}\exp^{-K'\ln^2(\lambda_{\rm max}/\lambda)}$; Serkowski, Mathewson, & Ford 1975) and find $\lambda_{\rm max}$=596 nm and $P_{\rm max}$=0.70% (K'=0.01+$\lambda_{\rm max}$/602). These values predict an interstellar polarization of 0.25% and 0.10% at 1.65 and 2.4μm respectively. Figure 3 shows the optical and near-infrared linear polarization values and the expected interstellar polarization. The mean linear polarization is 0.47±0.05% and 1.3±0.10% at 1.65μm and 2.4μm respectively. Although the optical polarization may be described as interstellar, the H and K-band polarization clearly cannot. The overall optical and near-infrared polarization spectrum can be described by two components; an interstellar polarization spectrum in the optical, and another component which dominates the H and K-band polarization spectrum. It should be noted that recent broad-band JHK measurements of polarization of Sco X-1 agree with the values we obtain here (Russell & Fender 2007). Given that Sco X–1 is known to be a powerful and variable jet source (Fomalont, Geldzahler, & Bradshaw 2001) the component in the IR is most likely due to optically thin synchrotron emission from the jet (see section 5). We can compare the near-infrared position angles with the position angle in the radio images of Sco X–1. The mean position angle of the radio jet on the sky is 54 degrees (Fomalont, Geldzahler, & Bradshaw 2001). This is approximately perpendicular to the near-infrared

electric vector position angle which implies that the magnetic field is aligned with the jet (assuming optically thin synchrotron emission).

4.2. *Cyg X–2*

Although polarization observations of Cyg X–2 are limited, optical linear measurements show Cyg X–2 to be 0.29% polarized, most of which may be intrinsic to the source (Koch Miramond & Naylor 1995). Our IR linear polarization measurements of 1.7% and 5.4% at 1.65μm and 2.4μm respectively show a considerable excess in the near-infrared compared to the optical. It is clear that interstellar polarization cannot explain the observed optical and near-infrared polarization values. The optical position angle of 36 degrees (Koch Miramond & Naylor 1995) differs from our near-infrared value, however, this can be explained if the jet evolves with time. The different position angles at 1.65μm and 2.4μm can be explained if the different bands come from different regions. For a 'simple' conical jet, the jet size scales with wavelength, so a 2.4μm jet would be (2.4/1.65) times larger than a 1.65μm jet. Cyg X–2, like Sco X–1, is a radio source (see Migliari & Fender 2006) and a member of the 'Z-source' and as such is also very likely to be a jet source (although one has never been spatially resolved).

4.3. *GRS 1915+105*

GRS 1915+105 is a powerful relativistic jet source (Mirabel & Rodriguez 1994; Fender et al. 1999; Miller-Jones et al. 2005) and the single most convincing example of IR synchrotron emission, with IR flare like events unambiguously associated with similar events at millimetre and radio wavelengths (e.g. Fender et al. 1997; Mirabel et al. 1998; Eikenberry et al. 1998b; Fender & Pooley 2000). However, at the time of the observations, radio monitoring with the Ryle Telescope at 15 GHz (Guy Pooley, private communication) indicated a low level of activity, with flux densities ≤ 10 mJy.

Our near-infrared linear polarization measurements of 7.5% and 5.0% at 1.65μm and 2.4μm may in fact be consistent with interstellar polarization, given the very high degree of extinction (Chapuis & Corbel 2004). However, we can estimate the maximum amount of interstellar polarization, given that there is a good correlation between the interstellar extinction and optical depth and thus polarization at 2.2μm for field stars (Jones 1989). For GRS 1915+105 the extinction of $E(B-V)$=6.3 (or A_v=19.5 mags; Chapuis & Corbel 2004) gives an optical depth of $\tau_{2.2\mu m} \sim 1.7$ and so a maximum interstellar polarization of $p_{2.2\mu m}$=3.3%. The observed polarization at 2.2μm of 3.7±1.1% (calculated using the mean value over 0.10μm) suggests that the observed polarization may in fact be consistent with interstellar polarization. However, if the dust induced polarization contribution is low, then the radio jets (mean position angle of ∼143 degrees; Miller-Jones et al. 2005) is perpendicular to the electric near-infrared vector postion angle, implying that the magnetic field is aligned with the jet.

5. POLARIZATION FROM JETS?

In X-ray binaries significant linear polarization caused by electron scattering in an isotropic medium (e.g. the environment of the accretion flow) is expected at optical wavelengths. Indeed the linear polarization property of the microquasar GRO J1655–40 in quiescence may be explained by such a mechanism (Scaltriti et al. 1997), where the linear polarization originates from asymmetrical regions in the inner accretion disc (electron scattering of the disc radiation by the secondary star is insignificant, because the secondary stars in LMXBs have low surface temperatures and therefore low free electron densities). In the case of the persistent LMXBs where the accretion disc dominates the optical light, the linear polarization should have a component that is produced by electron scattering by plasma above the accretion disc. Although a strong interstellar component is present, for Rayleigh and Thompson scattering processes, the level of linear polarization decreases as a function of increasing wavelength.

An excess weak component in the optical polarization is detected in Sco X–1 (Schultz et al. 2004), which is most likely due to electron scattering in the accretion disc. Similarly, for Cyg X–2 the optical polarization level has been measured to be 0.28%, which may be intrinsic to the source. However, we find the 2.4μm linear polarization level to be considerably larger compared to the optical and so the 2.4μm polarization cannot be explained by interstellar polarization or by electron scattering. In both of these sources therefore there seems to be some intrinsic polarization of the near-infrared which probably cannot be attributed to electron scattering. In the case of GRS 1915+105 the level of polarization is high but it does show the trend expected for interstellar scattering.

An alternative possibility is that the 'excess' near-infrared polarization is due to synchrotron emission from jets. Two polarization signatures are expected from the jet, depending on whether or not the synchrotron emission is optically thick or thin. Above some frequency this flat spectral component should break to an optically thin spectrum ($\alpha \sim -0.6$; $S_\nu \propto \nu^\alpha$) corresponding to the point at which the entire jet becomes transparent; i.e. emission at the break frequency arises primarily from the 'base' of the jet (although this may be still physically separated from the central accretor). For the optically thick part of the spectrum, which results in the flat spectral component ($\alpha \sim 0$) observed in the hard X-ray state (Fender 2001), no more than a few % polarization is expected. This is indeed observed for at least two hard state black hole sources in the radio band (see Fender 2001) – however such a low level of polarization would be very hard to distinguish from the similar levels expected from scattering in an accretion disc and/or by the interstellar medium.

There exists the possibility of a large fractional polarization level from optically thin synchrotron emission. While it is by no means firmly established, a small number of observational and theoretical results suggest a break between optically thick and thin emission should occur around the near-infrared band (e.g. see Corbel & Fender 2002). Optically thick synchrotron emission has a maximum linear polarization of ∼10% (Blandford et al. 2002), whereas optically thin synchrotron emission can have a fractional linear polarization as high as 70% (Blandford et al. 2002), where the observed level is generally significantly less than this due to a mixing of regions with different magnetic field

orientations and/or Faraday rotations within one resolution element of the telescope. Nevertheless, some X-ray binary jets show up to $\sim 30\%$ polarization (Fender 2001), indicating a highly significant ordering of the magnetic field. Figure 4 illustrates in more detail our expectation for the intrinsic (i.e. before interstellar scattering) linear polarization signature in the near-infrared and optical regimes, based on spectral energy distributions published in Corbel & Fender (2002) and Homan et al. (2005) and the simple ideas outlined above about the expected polarization fraction. At long wavelengths (maybe in the mid-infrared: the break is hard to determine precisely) there will only be $\sim 1\%$ polarization from the self-absorbed jet; at short wavelengths a comparable level will be measured due to scattering in the accretion flow. However, in the relatively narrow spectral region in which optically thin synchrotron emission dominates, we may expect a strong signature which initially rises to longer wavelengths as the relative jet:disc fraction increases. However, it should be noted that the break from optically thick to optically thin synchrotron and the normalisation of the disc component may vary from source to source, which will mean the width and peak of the high-polarization regime will vary. This is discussed in Nowak et al. (2005) for the case of black hole sources and clearly illustrated by Migliari et al. (2006) for the case of the neutron star 4U 0614+091 where the break to optically thin synchrotron appears to occur at a lower frequncy than what is measured for the black hole source GX 339-4 in Corbel & Fender (2002). Therefore the sketch in figure 4 can only be regarded as schematic.

Given that the 2.4μm polarization level is greater than the 1.65μm polarization level suggests that the most likely origin of the K-band linear polarization in Sco X–1 and Cyg X–2 is from a jet. Why the degree of polarization should be different by an order of magnitude between the two neutron star systems is unclear, but may relate to the accretion state (i.e. branch of the 'Z') the sources were on at the time (some branches seem to be more closely associated with jets than others, e.g. Migliari & Fender 2006). These observations support the recent discovery with *Spitzer* of optically thin synchrotron emission in the IR band from another neutron star X-ray binary, 4U 0614+091 (Migliari et al. 2006). In the case of GRS 1915+105 the result is ambiguous and further observations will be required to see how it might vary in states when the jet is more powerful (as indicated by e.g. simultaneous radio observations).

For Sco X–1 we find that the magnetic field is aligned with the jet (see section 4.1), and the same for GRS 1915+105 if the dust induced polarisation contribution is low (see section 4.3). Both parallel and perpendicular magnetic fields are seen in radio jets. In the radio polarization maps of Cir X–1 one observes the polarization vector rotate through 90 degrees between the core and the jet (Fender et al. 2007). Parallel magnetic fields are related to the intrinsic jet structure, perhaps helping to collimate the flow, whereas perpendicular magnetic fields indicate shocks, where the outflow is compressed along the jets axis (Saikia & Salter 1988). Measurements of the linear polarization of the compact jet in the near-infrared can probe closer to the central black hole or neutron star than the radio band, and reveal the degree or ordering of the magnetic field close to the jets's base. Furthermore, Faraday rotation (which is proportional to λ^2) is insignificant at near-infrared wavelengths, so that the linear polarization electic vector position angle tells us directly about the orientiation of the magnetic field (the two are perpendicular). The three measurements reported here, at least two of which indicate a significant contribution of synchrotron emission in the near-infrared, should be the beginning of a highly useful line of enquiry in the near future.

We would like to thank Chris Davis and Brad Cavanagh for help and discussions with the data reduction. We are also grateful to the referee for his/her careful reading of the paper. TS acknowledges support from the Spanish Ministry of Science and Technology under the programme Ramón y Cajal. CAW is supported by a PPARC Postdoctoral Fellowship. The United Kingdom Infrared Telescope is operated by the Joint Astronomy Centre on behalf of the U.K. Particle Physics and Astronomy Research Council. We thank the Department of Physical Sciences, University of Hertfordshire for providing IRPOL2 for the UKIRT.

REFERENCES

Bandyopadhyay, R. M., Shahbaz, T., Charles P. A., Naylor T., 1999, MNRAS, 306, 417
Blandford, R. D., Konigl, A., 1979, ApJ, 232, 34
Blandford R., Agol E., Broderick A., Heyl J., Koopmans L., Lee H.-W., 2002, in Astrophysical spectropolarimetry. Proceedings of the XII Canary Islands Winter School of Astrophysics, 177 (astro-ph/0107228)
Chapuis, C., Corbel, S., 2004, A&A, 414, 659
Corbel, S., Fender, R. P., 2002, ApJ, 573, L35
Eikenberry, S. S., Matthews, K., Murphy, T. W. Jr, Nelson, R. W., Morgan, E. H., Remillard, R. A., Muno, M., 1998b, ApJ, 506, L31
Fender, R. P., Pooley, G. G., Brocksopp, C., Newell, S. J., 1997, MNRAS, 290, L65
Fender, R. P., Garrington, S. T., McKay, D. J., Muxlow, T. W. B., Pooley, G. G., Spencer, R. E., Stirling, A. M., Waltman, E. B., 1999, MNRAS, 304, 865
Fender, R. P., Pooley, G. G., 2000, MNRAS, 318, L1
Fender, R. P., 2001, MNRAS, 322, 31
Fender, R., Wu K., Johnston, H., Tzioumis, T., Jonker, P., Spencer, R., van der Klis, M., 2004, Nature, 427, 222
Fender R. P., 2006, in Compact Stellar X-ray Sources, ed W.H.G., Lewin & M., van der Klis (Cambridge: Cambridge University Press), chapter 4, astro-ph/030339
Fender, R. P., et al., 2007, in prep
Fomalont, E. B., Geldzahler, B. J., Bradshaw, C. F., 2001, ApJ, 553, L27
Gehrels T., 1974, in Planets, stars and nebulae studied with photopolarimetry University of Arizona Press, Tucson
Homan, J., Buxton, M., Markoff, S., Bailyn, C. D., Nespoli, E., Belloni, T., 2005, ApJ, 624, 295
Howarth, I. D., 1983, MNRAS, 203, 301
Jensen, E. L. N., Mathieu, R. D., Donar, A. X., Dullighan, A., 2004, ApJ, 600, 789
Jones, T. J., 1989, ApJ, 346, 728
Koch Miramond, L., Naylor, T., 1995, A&A, 296, 390
Lazzati, D., et al. 2003, A&A, 410, 823
Markoff, S., Falcke, H., Fender, R.P., 2001, A&A, 372, L25
Markoff, S., Nowak, M., Corbel, S., Fender, R. P, Falcke, H., 2003, 397, 645
Migliari, S., Tomsick, J. A., Maccarone, T. J., Gallo, E., Fender, R. P., Nelemans, G., Russell, D. M., 2006, ApJ, 643, L41

Migliari, S., Fender, R. P., 2006, MNRAS, 366, 79
Miller-Jones, J. C. A., McCormick D. G., Fender, R. P., Spencer, R. E., Muxlow, T. W. B., Pooley, G. G., 2005, MNRAS, 363, 867
Mirabel, I. F., Rodriguez, L. F., 1994, 371, 46
Mirabel, I. F., Dhawan, V., Chaty, S., Rodriguez, L. F., Marti, J., Robinson, C. R., Swank, J., Geballe, T., 1998, A&A, 330, L9
Nowak, M. A., Wilms, J., Heinz, S., Pooley, G., Pottschmidt, K., Corbel,S., 2005, ApJ, 626, 1006
Orosz, J. A., Kuulkers, E., 1999, MNRAS, 305, 132
Pacholczyk A. G., 1977, in Radio galaxies: Radiation transfer, dynamics, stability and evolution of a synchrotron plasmon, Oxford Pergamon Press International Series on Natural Philosophy 89.
Russell, D. M., Fender, R.P , Hynes, R. I., Brocksopp, C., Homan, J., Jonker, P.G., Buxton, M.M ., 2006, MNRAS, in press, preprint (astro-ph/0606721)
Russell, D. M., Fender, R.P , 2007, MNRAS, submitted
Saikia, D. J., Salter, C. J., 1988, ARA&A, 26, 93
Scaltriti, F., Bodo, G., Ghisellini, G., Gliozzi, M., Trussoni, E., 1997, A&A, 325, L29
Schultz, J., Hakala, P., Huovelin, J., 2004, BaltA, 13, 581
Serkowski, K., Mathewson, D. L., Ford, V. L., 1975, ApJ, 196, 261
Simmons, J. F. L., Stewart, B. G., 1985, A&A, 142, 100
Vrtilek, S. D., Penninx, W., Raymond, J. C., Verbunt, F., Hertz, P., Wood, K., Lewin, W. H. G., Mitsuda, K., 1991, ApJ, 376, 278

TABLE 1
LOG OF OBSERVATIONS

Date	Object	UT Start	Exp. time	Comments
18 July	HIP79813	07:48	8×3 s	telluric F0V
	Sco X–1	08:32	16×300 s	
	HD144287	09:22	8×7 s	non-pol stnd
	HD183143	09:59	8×1 s	pol. stnd
19 July	HIP79813	07:48	8×3 s	telluric F0V
	Sco X–1	08:01	8×300 s	
	HD144287	09:18	8×7 s	non-pol. stdn
	HD183143	09:52	8×1 s	pol. star
	HIP95002	10:11	8×3 s	telluric A2V
	GRS 1915+105	10:21	16×240 s	
22 July	Cyg X–2	08:32	24×240 s	
	HIP107253	11:01	8×3 s	telluric A0V
	HD198478	12:58	8×7 s	non-pol. stnd
	HD183143	12:51	8×1 s	pol. star
23 July	HIP79813	05:33	8×3 s	telluric F0V
	Sco X–1	05:40	16×300 s	
	HD144287	07:14	8×7 s	non-pol. stnd
	HD183143	07:29	8×1 s	pol. stnd

TABLE 2
POLARIMETRY RESULTS. THE 1.65μM AND 2.4μM PERCENTAGE POLARIZATION (p), POSITION ANGLE (θ) AND DEREDDENED FLUX DENSITIES (I) ARE CALCULATED USING MEAN VALUES OVER 0.10μM.

Object	UT date	1.65μm p(%)	θ(°)	I(mJy)
		2.40μm p(%)	θ(°)	I(mJy)
Sco X–1	20040718	0.38±0.04	136±2	21±2
		0.93±0.05	147±3	15±1
	20040723	0.67±0.04	116±2	32±2
		1.14±0.06	129±3	22±2
Cyg X–2	20040722	1.7±0.2	96±2	6.4±0.4
		5.4±0.7	84±3	4.3±0.2
GRS 1915+105	20040719	7.9±1.0	49±2	29±3
		5.0±1.2	50±3	15±2

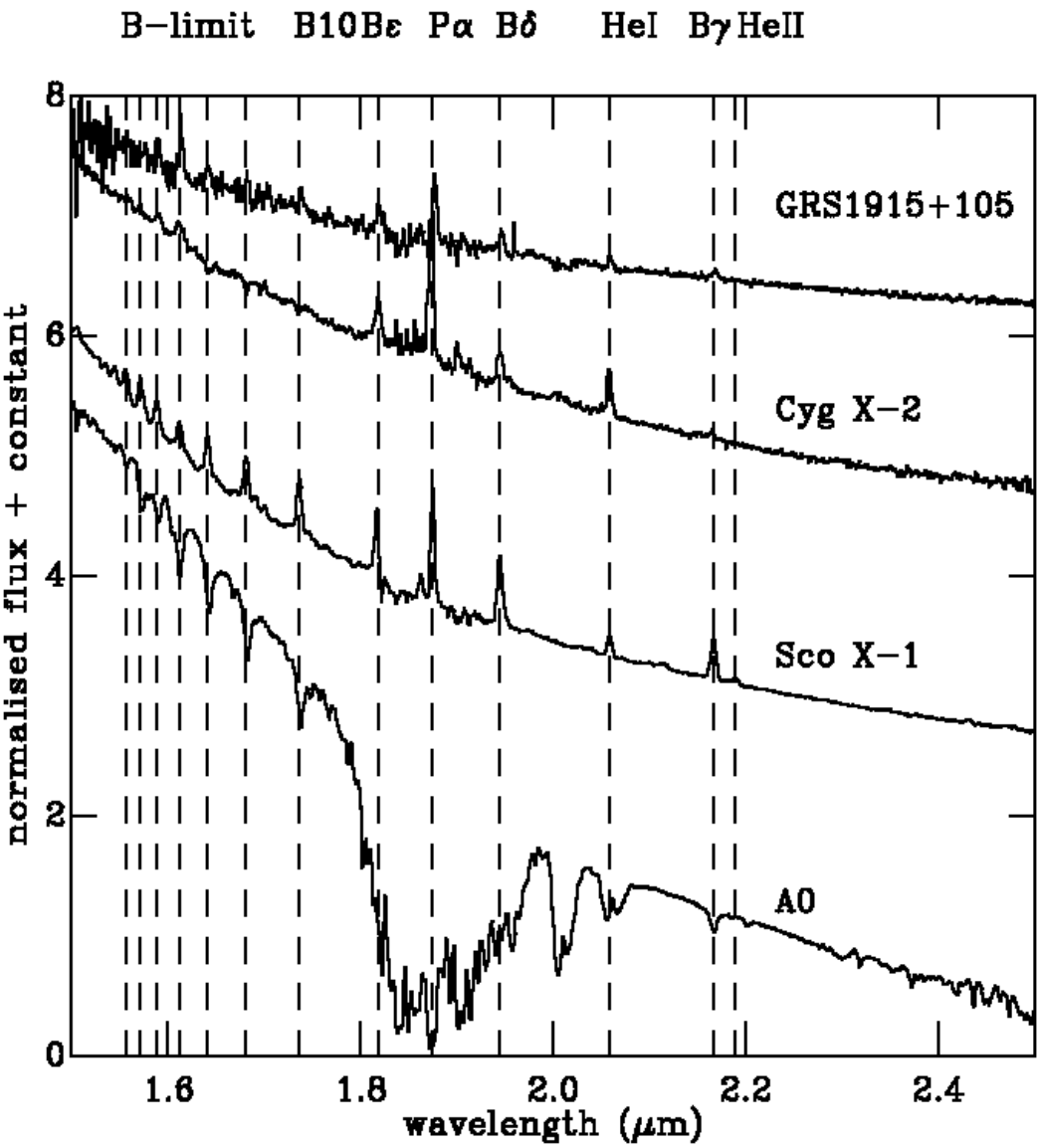

FIG. 1.— The dereddened HK spectrum of Sco X–1, Cyg X–2 and GRS 1915+105. The spectrum of a telluric A0-star is also shown. The spectra have been normalised by dividing by the flux at 2.25 μm and then offset on the y-axis by adding a multiple of 1 to each spectrum.

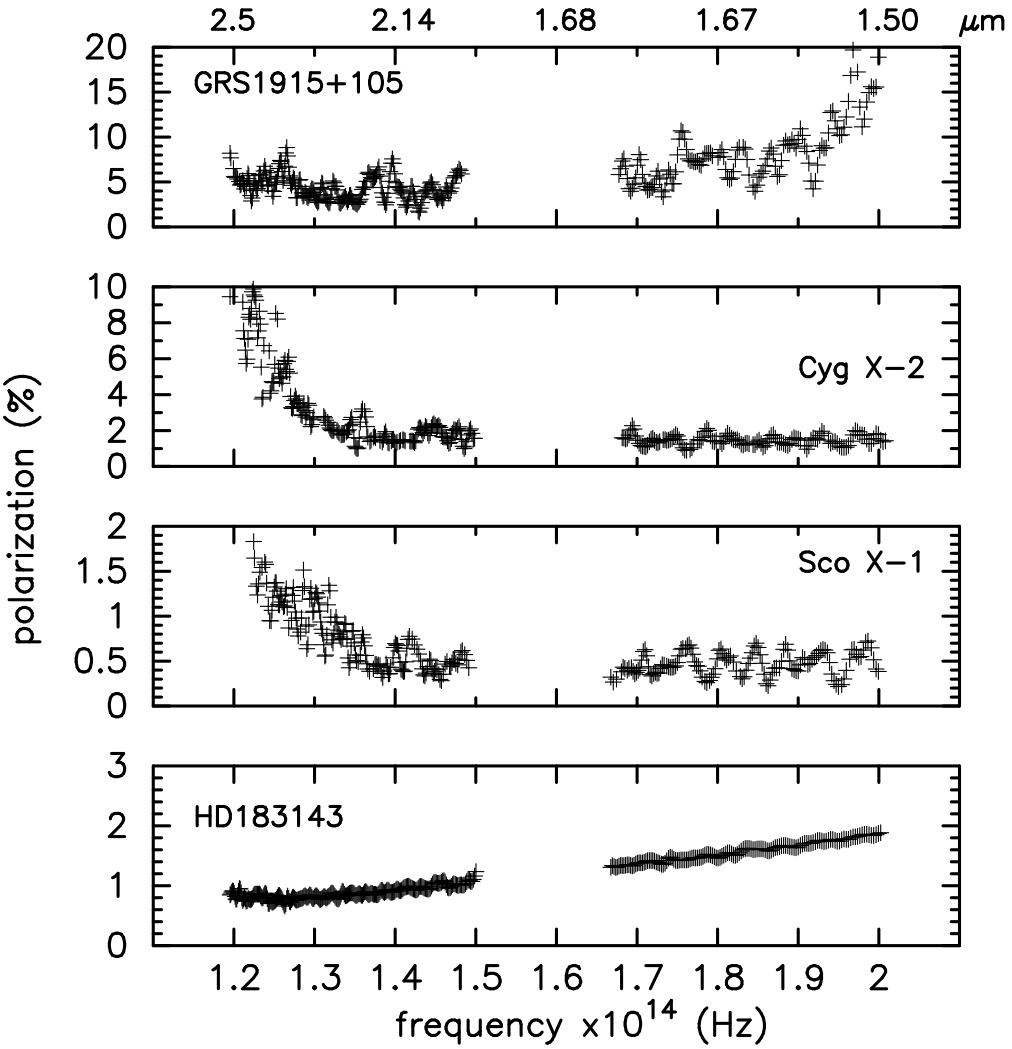

FIG. 2.— From top to bottom: the HK linear polarization spectrum of GRS 1915+05, Cyg X–2, Sco X–1 and the polarized standard star HD184143. The gap in the spectra between 1.8 and 2.0μm is the atmospheric absorption band.

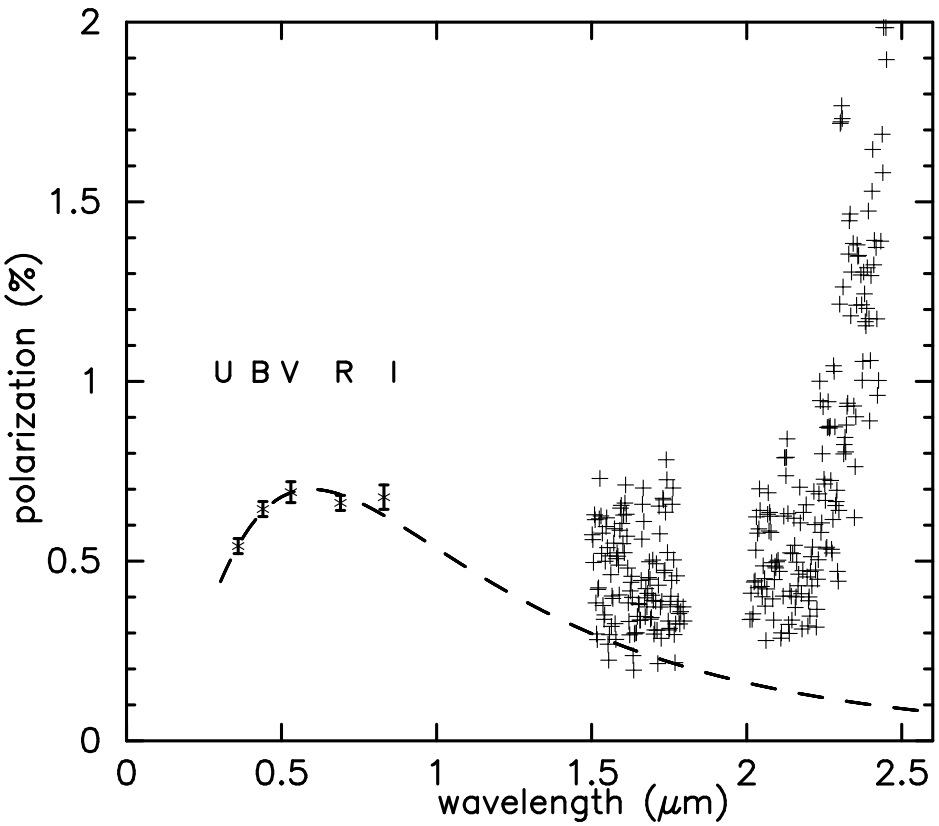

FIG. 3.— The optical and near-infrared polarization values for Sco X–1. The optical points (stars) are taken from Schultz et al. (2004) and our HK polarization spectrum (crosses) is shown. The dashed line is the interstellar polarization model fit to the optical.

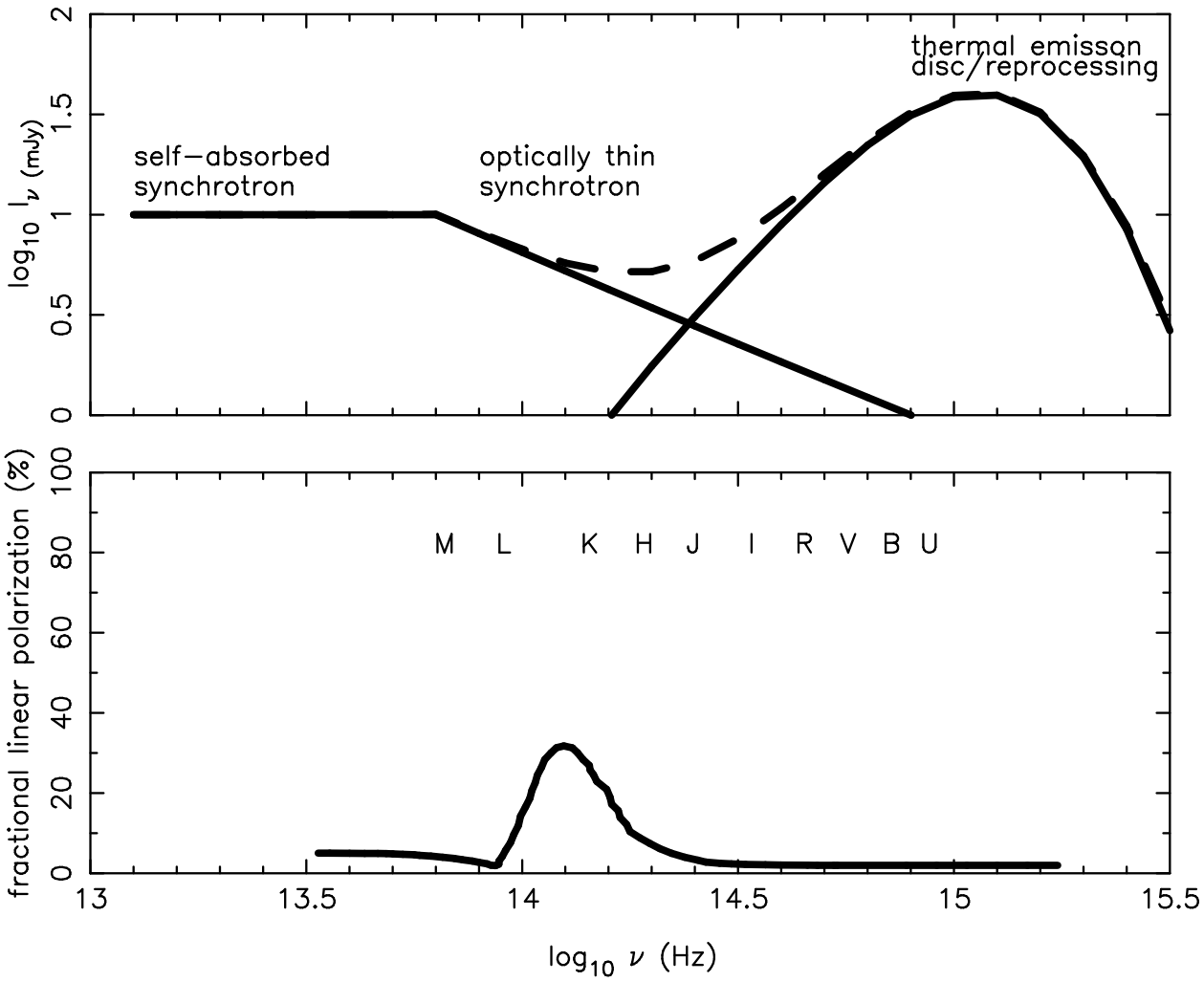

FIG. 4.— Expectations for the linear polarization signature in the near-infrared and optical regimes of X-ray binaries. The dashed line shows the observed spectral energy distribution. The linear polarization due to optically thick of thin synchrotron emission is frequency dependant (Pacholczyk 1977). The key spectral points are the break from optically thick (low polarization <10%) to optically thin (high polarization <70%) synchrotron emission, and the point at which the thermal (low polarization) emission begins to dominate over the jet. These effects should combine to produce a narrow spectral region with relatively high linear polarization arising from close to the base of the jet.